Appl Phys B (2011) 105:285–291
DOI 10.1007/s00340-011-4692-z

Applied Physics B
Lasers and Optics

Target-in-the-loop high-power adaptive phase-locked fiber laser array using single-frequency dithering technique

R. Tao · Y. Ma · L. Si · X. Dong · P. Zhou · Z. Liu

Received: 22 January 2011 / Revised version: 21 May 2011 / Published online: 1 September 2011

Abstract We present a theoretical and experimental study of a target-in-the-loop (TIL) high-power adaptive phase-locked fiber laser array. The system configuration of the TIL adaptive phase-locked fiber laser array is introduced, and the fundamental theory for TIL based on the single-dithering technique is deduced for the first time. Two 10-W-level high-power fiber amplifiers are set up and adaptive phase locking of the two fiber amplifiers is accomplished successfully by implementing a single-dithering algorithm on a signal processor. The experimental results demonstrate that the optical phase noise for each beam channel can be effectively compensated by the TIL adaptive optics system under high-power applications and the fringe contrast on a remotely located extended target is advanced from 12% to 74% for the two 10-W-level fiber amplifiers.

1 Introduction

Fiber lasers have wide potential for applications due to their essential characters such as high conversion efficiency, excellent beam quality, convenient heat management, and compact configuration [1]. With the development of high-power laser diode pumped technology and double-clad fiber production crafts, the output power of fiber lasers is increasing at a great speed in recent years. But, the ultimate output power of a single fiber laser is limited due to nonlinear effects, facet fracture, and thermal lensing [2]. Coherent beam combining of fiber lasers/amplifiers, which provides an effective approach not only for achieving a high-power laser beam with good beam quality but also for convenient heat management, has been under intensive research recently [3–12]. Nevertheless, previous investigation of coherent beam combining mainly focused on phase locking of the fiber laser array in an experimental environment; only phase noise induced by fiber amplifiers needs to be corrected. In a real application scheme, the effect of atmospheric turbulence on the combined beam must be considered. The propagation of a fiber laser array beam will inevitably be affected by atmospheric turbulence and the mutual coherence could even be destroyed [13–16]. For a real high energy laser system built on a coherently combined fiber laser array, mitigation of the effect of the atmosphere on laser beam propagation is a key problem to be solved urgently. A laser beam control technique, which could be called the target-in-the-loop (TIL) control concept, provides a novel approach to solve this problem [17–20]. In 2002, Vorontsov and Carhart accomplished a TIL adaptive phase distortion correction experiment based on the stochastic parallel gradient descent (SPGD) optimization method at a low operation power level; it is shown that the TIL control can significantly improve laser beam concentration on extended objects [21]. The signal from the target used for phase locking is obtained by using a telescope and a CCD. A similar study of TIL control but based on a multi-dithering technique or self-referenced locking of optical coherence by a single-detector electronic-frequency tagging (LOCSET) method has been accomplished by Jolivet et al. with three 2-W fiber amplifiers [22]. The signal from the target used for phase locking is obtained by using a polarization beam splitter (PBS) cube and a photodetector.

In the present paper, we will demonstrate the TIL adaptive phase locking of a high-power fiber laser array using the single-dithering technique [23], which had been demonstrated to have great potential in scaling to a large number of

R. Tao · Y. Ma · L. Si · X. Dong · P. Zhou (✉) · Z. Liu
College of Optoelectric Science and Engineering, National University of Defense Technology, Changsha 410073, China
e-mail: zhoupu203@163.com

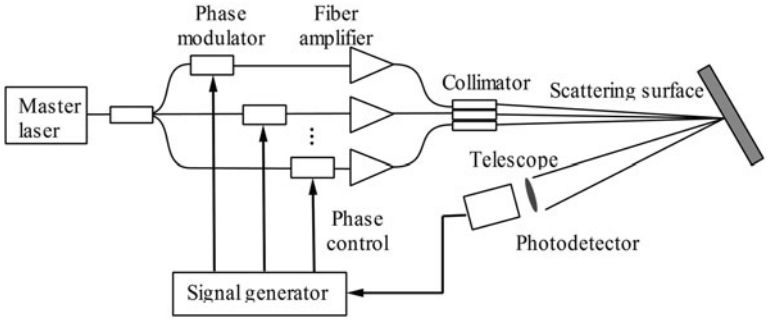

Fig. 1 Schematic diagram of TIL

beamlets with a simple phase-control system and low cost. We get the signal from the target used for phase locking by using a telescope and a photodetector, which eliminates the complexity and difficulty in beam aligning when using the PBS, and the employment of the photodetector will greatly improve the system working bandwidth compared with using a CCD because of its faster response. A two-10-W-level high-power fiber laser array is successfully phase locked in the TIL configuration.

2 Analysis of theory

A typical schematic of the TIL adaptive phase-locked fiber laser array is shown in Fig. 1 [24]. The master laser is split into N channels. Each channel is modulated respectively with same-frequency little-amplitude sine waves but at different time intervals. Then the N beams are amplified by the fiber amplifiers respectively and coherently combined on a remotely located extended scattering surface. A telescope acting as the receiver system is located next to the fiber laser array and the photodectector is placed just behind the telescope.

By taking into account both propagation through turbulence and presence of a scattering target in the loop, the basic theory for phase locking of a fiber laser array in TIL configuration can be given as follows [22, 23, 25].

Assuming that the optical fields of all beams are plane waves, the fields of beam i that are not phase modulated, $E_i(t)$, are given by

$$E_i(t) = E_{i0}\cos(\omega_{\mathrm{L}}t + \phi_i) \quad (\text{where } i = 1, 2, 3, \ldots, N), \quad (1)$$

where E_{i0} and ϕ_i represent the field amplitude and the optical phase of the beam i, and ω_{L} represents the laser frequency.

During different time intervals, the same modulation signal is added to a different beam channel j while all the other beams are unmodulated and the field of beam j can be written as

$$E_j(t) = E_{j0}\cos\big(\omega_{\mathrm{L}}t + \phi_j + \beta\sin(\omega t)\big) \quad (\text{where } j = 1, 2, 3, \ldots, N), \quad (2)$$

where β and ω are the phase modulation amplitude and frequency, respectively.

For a remotely located extended target, light from a small scattering area will be collimated in different directions. The telescope selects a certain direction of rays so that all the optical rays of a given scattering area will pass through the same cylindrical channel whatever direction the laser beam originates from. If the diameter of the telescope is smaller than Fried's diameter of the atmospheric turbulence, all the optical rays of a given propagation channel suffer from the same backward-turbulence-induced phase shift. $\Delta\phi_{\mathrm{bs}}$ denotes the backward-turbulence-induced phase shift of the rays scattered from the area s, where s refers to the contributing scattering areas which are present in the laser-illuminated area, and $s = 1, 2, 3, \ldots, M$. The unmodulated optical fields $E_{s\_i}(t)$ and the modulated optical fields $E^m_{s\_j}(t)$ backscattered by the sth scattering area can be written as

$$E_{s\_i}(t) = \eta_s E_{i0}\cos(\omega_{\mathrm{L}}t + \phi_i + \Delta\phi_{if} + \varphi_s + \Delta\phi_{bs}) \quad (\text{where } i = 1, 2, 3, \ldots, j-1, j+1, \ldots, N) \quad (3)$$

and

$$E^m_{s\_j}(t) = \eta_s E_{j0}\cos(\omega_{\mathrm{L}}t + \phi_j + \beta\sin(\omega t) + \Delta\phi_{jf} + \varphi_s + \Delta\phi_{bs}) \quad (\text{where } j = 1, 2, 3, \ldots, N), \quad (4)$$

where η_s and φ_s stand for the scattering index and phase shift of the sth scattering area, $\Delta\phi_{if}$ stands for the onward-turbulence-induced uniform phase difference of beam i, and it is assumed that the diameter of each beam is smaller than Fried's diameter to get $\Delta\phi_{if}$.

If the jth channel is modulated at moment t, the total optical intensity is given by

$$
\begin{aligned}
I_j(t) &= \left[\sum_{\substack{i=1\\ i\neq j}}^{N}\sum_{s=1}^{M} E_{s\_i}(t) + \sum_{s=1}^{M} E^m_{s\_j}(t)\right]^2 \\
&= \sum_{\substack{i=1\\ i\neq j}}^{N}\sum_{s=1}^{M}\left(E_{s\_i}(t)\right)^2 + \sum_{s=1}^{M}\left(E^m_{s\_j}(t)\right)^2 \\
&\quad + \sum_{s=1}^{M}\sum_{\substack{i=1\\ i\neq j}}^{N}\sum_{\substack{k=1\\ k\neq j\\ k\neq i}}^{N}\left(E_{s\_i}(t)E_{s\_k}(t)\right) \\
&\quad + \sum_{s=1}^{M}\sum_{\substack{r=1\\ r\neq s}}^{M}\sum_{\substack{i=1\\ i\neq j}}^{N}\left(E_{s\_i}(t)E_{r\_i}(t)\right) \\
&\quad + \sum_{s=1}^{M}\sum_{\substack{r=1\\ r\neq s}}^{M}\sum_{\substack{i=1\\ i\neq j}}^{N}\sum_{\substack{k=1\\ k\neq j\\ k\neq i}}^{N}\left(E_{s\_i}(t)E_{r\_k}(t)\right) \\
&\quad + \sum_{r=1}^{M}\sum_{\substack{s=1\\ s\neq r}}^{M}\left(E^m_{s\_j}(t)E^m_{r\_j}(t)\right) \\
&\quad + 2\sum_{s=1}^{M}\sum_{\substack{i=1\\ i\neq j}}^{N}\sum_{r=1}^{M} E_{s\_i}(t)E^m_{r\_j}(t) \qquad (5)
\end{aligned}
$$

with

$$
\begin{aligned}
&\sum_{s=1}^{M}\sum_{\substack{i=1\\ i\neq j}}^{N}\sum_{\substack{k=1\\ k\neq j\\ k\neq i}}^{N}\left(E_{s\_i}(t)E_{s\_k}(t)\right) \\
&= \sum_{s=1}^{M}\sum_{\substack{i=1\\ i\neq j}}^{N}\sum_{\substack{k=1\\ k\neq j\\ k\neq i}}^{N}\left\{\begin{array}{l}\eta_s^2 E_{i0}E_{k0}\cos(\omega_{\mathrm{L}}t+\phi_i+\Delta\phi_{if}\\ \quad+\varphi_s+\Delta\phi_{bs})\cos(\omega_{\mathrm{L}}t+\phi_k\\ \quad+\Delta\phi_{kf}+\varphi_s+\Delta\phi_{bs})\end{array}\right\}, \qquad (6)
\end{aligned}
$$

$$
\begin{aligned}
&\sum_{s=1}^{M}\sum_{\substack{r=1\\ r\neq s}}^{M}\sum_{\substack{i=1\\ i\neq j}}^{N}\left(E_{s\_i}(t)E_{r\_i}(t)\right) \\
&= \sum_{s=1}^{M}\sum_{\substack{r=1\\ r\neq s}}^{M}\sum_{\substack{i=1\\ i\neq j}}^{N}\left\{\begin{array}{l}\eta_s\eta_r E_{i0}E_{i0}\cos(\omega_{\mathrm{L}}t+\phi_i+\Delta\phi_{if}\\ \quad+\varphi_s+\Delta\phi_{bs})\cos(\omega_{\mathrm{L}}t+\phi_i\\ \quad+\Delta\phi_{if}+\varphi_r+\Delta\phi_{br})\end{array}\right\}, \qquad (7)
\end{aligned}
$$

$$
\begin{aligned}
&\sum_{s=1}^{M}\sum_{\substack{r=1\\ r\neq s}}^{M}\sum_{\substack{i=1\\ i\neq j}}^{N}\sum_{\substack{k=1\\ k\neq j\\ k\neq i}}^{N}\left(E_{s\_i}(t)E_{r\_k}(t)\right) \\
&= \sum_{s=1}^{M}\sum_{\substack{r=1\\ r\neq s}}^{M}\sum_{\substack{i=1\\ i\neq j}}^{N}\sum_{\substack{k=1\\ k\neq j\\ k\neq i}}^{N}\left\{\begin{array}{l}\eta_s\eta_r E_{i0}E_{i0}\cos(\omega_{\mathrm{L}}t+\phi_i\\ \quad+\Delta\phi_{if}+\varphi_s+\Delta\phi_{bs})\\ \quad\times\cos(\omega_{\mathrm{L}}t+\phi_k+\Delta\phi_{kf}\\ \quad+\varphi_r+\Delta\phi_{br})\end{array}\right\}, \qquad (8)
\end{aligned}
$$

$$
\begin{aligned}
&\sum_{r=1}^{M}\sum_{\substack{s=1\\ s\neq r}}^{M}\left(E^m_{s\_j}(t)E^m_{r\_j}(t)\right) \\
&= \sum_{r=1}^{M}\sum_{\substack{s=1\\ s\neq r}}^{M}\left\{\begin{array}{l}\eta_s\eta_r (E_{j0})^2\cos(\omega_{\mathrm{L}}t+\phi_j+\beta\sin(\omega t)\\ \quad+\Delta\phi_{jf}+\varphi_s+\Delta\phi_{bs})\\ \quad\times\cos(\omega_{\mathrm{L}}t+\phi_j+\beta\sin(\omega t)\\ \quad+\Delta\phi_{jf}+\varphi_r+\Delta\phi_{br})\end{array}\right\}, \qquad (9)
\end{aligned}
$$

$$
\begin{aligned}
&\sum_{s=1}^{M}\sum_{\substack{i=1\\ i\neq j}}^{N}\sum_{r=1}^{M} E_{s\_i}(t)E^m_{r-j} \\
&= \sum_{s=1}^{M}\sum_{\substack{i=1\\ i\neq j}}^{N}\sum_{r=1}^{M}\left\{\begin{array}{l}\eta_s\eta_r E_{i0}E_{j0}\cos(\omega_{\mathrm{L}}t+\phi_i\\ \quad+\Delta\phi_{if}+\varphi_s+\Delta\phi_{bs})\\ \quad\times\cos(\omega_{\mathrm{L}}t+\phi_j+\beta\sin(\omega t)\\ \quad+\Delta\phi_{jf}+\varphi_r+\Delta\phi_{br})\end{array}\right\}. \qquad (10)
\end{aligned}
$$

Substituting (6), (7), (8), (9), and (10) into (5), using the trigonometric identity, we get

$$
\begin{aligned}
I_j(t) &= I_{j0} \\
&\quad + \sum_{s=1}^{M}\sum_{\substack{i=1\\ i\neq j}}^{N}\sum_{r=1}^{M}\left(\eta_s\eta_r E_{i0}E_{j0}\cos\left(\psi_{sr}-\beta\sin(\omega t)\right)\right) \\
&= I_{j0} + \sum_{s=1}^{M}\sum_{\substack{i=1\\ i\neq j}}^{N}\sum_{r=1}^{M}\left\{\begin{array}{l}\sqrt{P_{is}P_{jr}}\cos(\psi_{sr})\left[J_0(\beta)\right.\\ \quad\left.+2\left(\sum_{N_i=1}^{\infty}J_{2N_i}(\beta)\right.\right.\\ \quad\left.\left.\times\cos(2N_i\omega t)\right)\right]\\ \quad+2\sqrt{P_{is}P_{jr}}\sin(\psi_{sr})\\ \quad\times\left[\sum_{N_j=1}^{\infty}J_{2N_j-1}(\beta)\right.\\ \quad\left.\times\sin((2N_j-1)\omega t)\right]\end{array}\right\} \qquad (11)
\end{aligned}
$$

with

$$
\begin{aligned}
\psi_{sr} &= \phi_i-\phi_j+\Delta\phi_{if}-\Delta\phi_{jf} \\
&\quad +\varphi_s-\varphi_r+\Delta\phi_{bs}-\Delta\phi_{br}, \qquad (12)
\end{aligned}
$$

$$P_{is} = \eta_s^2 E_{i0}^2, \tag{13}$$

and

$$P_{jr} = \eta_r^2 E_{j0}^2, \tag{14}$$

where I_{j0} contains the light frequency terms that cannot be responded to by the photodetector and is treated as a direct-current term as a whole, P_{is} and P_{jr} are the optical power backscattered to the photodetector from the sth and rth scattering areas for the unmodulated beam and the jth-phase-modulated beam, respectively, and N_i, N_j are subscripts as a whole.

The second term of (11) can be written as

$$\sum_{s=1}^{M}\sum_{\substack{i=1\\ i\neq j}}^{N}\sum_{r=1}^{M} \times \left\{ \begin{array}{l} \sqrt{P_{is}P_{jr}}\cos(\psi_{sr}) \\ \quad \times \left[J_0(\beta) + 2\left(\sum_{N_i=1}^{\infty} J_{2N_i}(\beta)\cos(2N_i\omega t) \right) \right] \\ \quad + 2\sqrt{P_{is}P_{jr}}\sin(\psi_{sr}) \\ \quad \times \left[\sum_{N_j=1}^{\infty} J_{2N_j-1}(\beta)\sin((2N_j-1)\omega t) \right] \end{array} \right\}$$

$$= \sum_{s=1}^{M}\sum_{\substack{i=1\\ i\neq j}}^{N} \left\{ \begin{array}{l} \sqrt{P_{is}P_{js}}\cos(\psi_{ss}) \\ \quad \times \left[J_0(\beta) + 2\left(\sum_{N_i=1}^{\infty} J_{2N_i}(\beta) \right.\right. \\ \quad \left.\left. \times \cos(2N_i\omega t) \right) \right] \\ \quad + 2\sqrt{P_{is}P_{js}}\sin(\psi_{ss}) \\ \quad \times \left[\sum_{N_j=1}^{\infty} J_{2N_j-1}(\beta)\sin((2N_j-1)\omega t) \right] \end{array} \right\}$$

$$+ \sum_{s=1}^{M}\sum_{\substack{i=1\\ i\neq j}}^{N}\sum_{\substack{r=1\\ r\neq s}}^{M} \left\{ \begin{array}{l} \sqrt{P_{is}P_{jr}}\cos(\psi_{sr}) \\ \quad \times \left[J_0(\beta) + 2\left(\sum_{N_i=1}^{\infty} J_{2N_i}(\beta) \right.\right. \\ \quad \left.\left. \times \cos(2N_i\omega t) \right) \right] \\ \quad + 2\sqrt{P_{is}P_{jr}}\sin(\psi_{sr}) \\ \quad \times \left[\sum_{N_j=1}^{\infty} J_{2N_j-1}(\beta) \right. \\ \quad \left. \sin((2N_j-1)\omega t) \right] \end{array} \right\}. \tag{15}$$

As $\psi_{ss} = \phi_i - \phi_j + \Delta\phi_{if} - \Delta\phi_{jf}$ for all s, the first term of (15) can be simplified into

$$\sum_{s=1}^{M}\sum_{\substack{i=1\\ i\neq j}}^{N} \left\{ \begin{array}{l} \sqrt{P_{is}P_{js}}\cos(\psi_{ss}) \\ \quad \times \left[J_0(\beta) + 2\left(\sum_{N_i=1}^{\infty} J_{2N_i}(\beta)\cos(2N_i\omega t) \right) \right] \\ \quad + 2\sqrt{P_{is}P_{js}}\sin(\psi_{ss}) \\ \quad \times \left[\sum_{N_j=1}^{\infty} J_{2N_j-1}(\beta)\sin((2N_j-1)\omega t) \right] \end{array} \right\}$$

$$= \left(\sum_{s=1}^{M} \eta_s \right) E_{j0}$$

$$\times \sum_{\substack{i=1\\ i\neq j}}^{N} \left\{ \begin{array}{l} E_{i0}\cos(\phi_i - \phi_j + \Delta\phi_{if} - \Delta\phi_{jf}) \left[J_0(\beta) \right. \\ \quad \left. + 2\left(\sum_{N_i=1}^{\infty} J_{2N_i}(\beta)\cos(2N_i\omega t) \right) \right] \\ \quad + 2E_{i0}\sin(\phi_i - \phi_j + \Delta\phi_{if} - \Delta\phi_{jf}) \\ \quad \times \left[\sum_{N_j=1}^{\infty} J_{2N_j-1}(\beta)\sin((2N_j-1)\omega t) \right] \end{array} \right\}, \tag{16}$$

where $\phi_i - \phi_j + \Delta\phi_{if} - \Delta\phi_{jf}$ is the phase difference originating from the laser amplifiers and onward-turbulence-induced phase fluctuations.

As for the second term of (15), it can be written as

$$\sum_{s=1}^{M}\sum_{\substack{i=1\\ i\neq j}}^{N}\sum_{\substack{r=1\\ r\neq s}}^{M} \left\{ \begin{array}{l} \sqrt{P_{is}P_{jr}}\cos(\psi_{sr}) \\ \quad \times \left[J_0(\beta) + 2\left(\sum_{N_i=1}^{\infty} J_{2N_i}(\beta) \right.\right. \\ \quad \left.\left. \times \cos(2N_i\omega t) \right) \right] \\ \quad + 2\sqrt{P_{is}P_{jr}}\sin(\psi_{sr}) \\ \quad \times \left[\sum_{N_j=1}^{\infty} J_{2N_j-1}(\beta)\sin((2N_j-1)\omega t) \right] \end{array} \right\}$$

$$
= \sum_{\substack{i=1 \\ i\neq j}}^{N} \left\{ \begin{array}{l} E_{i0}E_{j0}\cos(\phi_i - \phi_j + \Delta\phi_{if} - \Delta\phi_{jf}) \Bigg[J_0(\beta) \\ \quad + 2\left(\sum\limits_{N_i=1}^{\infty} J_{2N_i}(\beta)\cos(2N_i\omega t) \right) \Bigg] \sum\limits_{\cos} \\ \quad - E_{i0}E_{j0}\sin(\phi_i - \phi_j + \Delta\phi_{if} - \Delta\phi_{jf}) \\ \quad \Bigg[J_0(\beta) + 2\left(\sum\limits_{N_i=1}^{\infty} J_{2N_i}(\beta) \right. \\ \quad \left. \times \cos(2N_i\omega t) \right) \Bigg] \sum\limits_{\sin} \\ \quad + 2E_{i0}E_{j0}\sin(\phi_i - \phi_j + \Delta\phi_{if} - \Delta\phi_{jf}) \\ \quad \times \left[\sum\limits_{N_j=1}^{\infty} J_{2N_j-1}(\beta)\sin((2N_j-1)\omega t) \right] \sum\limits_{\cos} \\ \quad + 2E_{i0}E_{j0}\cos(\phi_i - \phi_j + \Delta\phi_{if} - \Delta\phi_{jf}) \\ \quad \times \left[\sum\limits_{N_j=1}^{\infty} J_{2N_j-1}(\beta)\sin((2N_j-1)\omega t) \right] \sum\limits_{\sin} \end{array} \right\} \tag{17}
$$

with

$$
\left\{ \begin{array}{l} \sum\limits_{\cos} = \sum\limits_{s=1}^{M} \sum\limits_{\substack{r=1 \\ r\neq s}}^{M} \sqrt{\eta_s \eta_r}\cos(\varphi_s - \varphi_r + \Delta\phi_{bs} - \Delta\phi_{br}), \\ \sum\limits_{\sin} = \sum\limits_{s=1}^{N} \sum\limits_{\substack{r=1 \\ r\neq s}}^{N} \sqrt{\eta_s \eta_r}\sin(\varphi_s - \varphi_r + \Delta\phi_{bs} - \Delta\phi_{br}). \end{array} \right. \tag{18}
$$

Assume that the scattering areas are uncorrelated [26] and the turbulence-induced phase shifts in two different channels of propagation are uncorrelated as well. So, $\varphi_s - \varphi_r + \Delta\phi_{bs} - \Delta\phi_{br}$ is a random variable with uniform distribution of probability over $[-\pi, \pi]$. η_s is also a random variable with average value η_{s0}.

Due to the small size of the telescope, the part of the target containing the scattering areas contributing to the signal, which has a surface inversely proportional to the telescope diameter, is wide and contains a large number of scattering areas. Therefore, we can derive that the values of $\sum_{\cos}$ and $\sum_{\sin}$ are normally distributed around their average values, which are here equal to zero, by applying the central limit theorem. Thus, $\sum_{\cos}$ and $\sum_{\sin}$ are both very close to zero and, with the highest probability, negligible when compared with the $\sum_{s=1}^{M} \eta_s$ term of (16) [22], so we can neglect the terms from (17) when compared with similar terms in (16).

The photodetector current is

$$
i_{j\mathrm{PD}}(t) = R_{\mathrm{PD}} \cdot S \cdot \sqrt{\frac{\varepsilon_0}{\mu_0}} \cdot I_j(t), \tag{19}
$$

where μ_0 and ε_0 represent the magnetic and electric permeabilities of free space, R_{PD} represents the responsivity of the photodetector, and S represents the photodetector area.

The phase-control signal is extracted from the photocurrent by demodulating. When the photocurrent is integrated over a time τ after being multiplied by $\sin(\omega t)$ and τ is long enough for integration but short enough for phase control, the phase error control signal of beam channel j is derived, which is given by

$$
\begin{aligned} S_j = {} & R_{\mathrm{PD}} \cdot J_1(\beta) \cdot S \cdot \sqrt{\frac{\varepsilon_0}{\mu_0}} \cdot \left(\sum_{s=1}^{M} \eta_s \right) \cdot E_{j0} \\ & \times \sum_{\substack{i=1 \\ i\neq j}}^{N} E_{i0}\sin(\phi_i - \phi_j + \Delta\phi_{if} - \Delta\phi_{jf}), \end{aligned} \tag{20}
$$

where J_1 is the Bessel function of the first kind of order one. This demonstrates that the phase-control signal only contains the phase differences originating from the laser amplifiers and onward-turbulence-induced phase fluctuations. Therefore, phase locking of the laser amplifiers on the plane of the scattering surface can be realized by compensating the error signal.

The phase error control signal of beam channel j is sent to the signal processing block and used for the phase control of beam channel j, while the phase control signals of the other channels hold the previous phase control signal. Then the phases of the N beams could be locked by repeating the above operations for the different channels in turn and the TIL phase locking on the remotely located extended target thus can be realized successfully.

3 Experimental setup and results

The basic experimental setup is shown in Fig. 2. A single-frequency fiber laser with 1064-nm wavelength is provided as the fiber laser. The line width of the single-frequency fiber laser is narrower than 20 kHz. The seed laser is split into two channels (A and B) by using a single mode coupler. In each channel, we build a cascaded two-stage fiber amplifier to boost the laser power to 10-W level. In the main amplification stage, a 5-m-long double-clad Yb-doped fiber with 11-μm core diameter and 130-μm inner clad diameter is employed. Two 9-W-level laser diodes (LDs) are used to pump the main amplifier stage via a $(6 + 1) \times 1$ pump combiner (only two pump ports are employed).

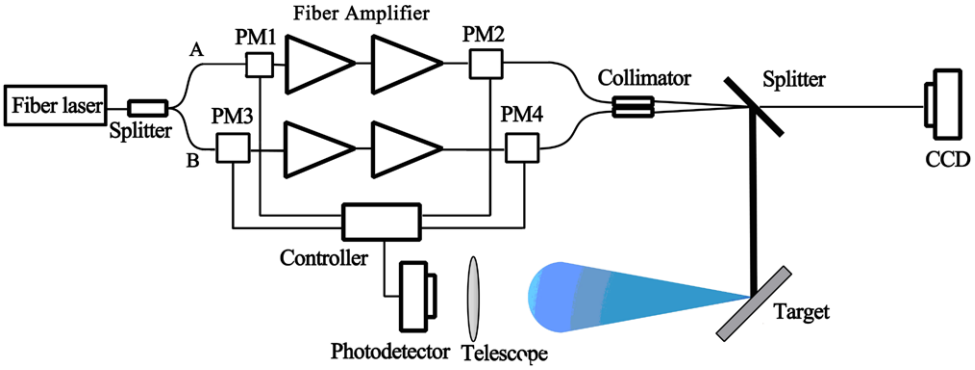

Fig. 2 Experimental setup for the TIL system

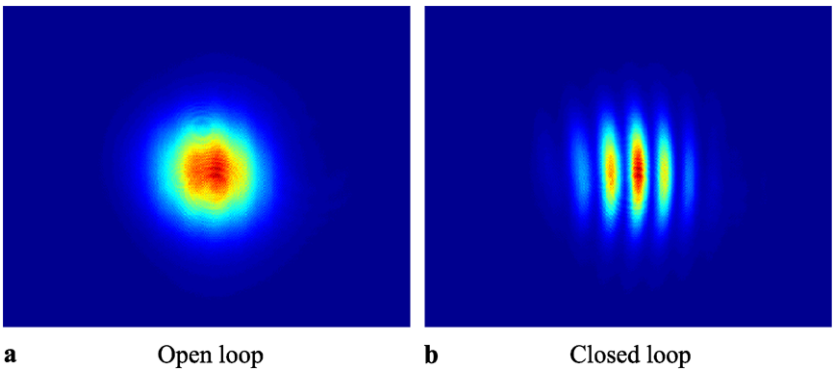

Fig. 3 Far-field intensity patterns for open loop and closed loop

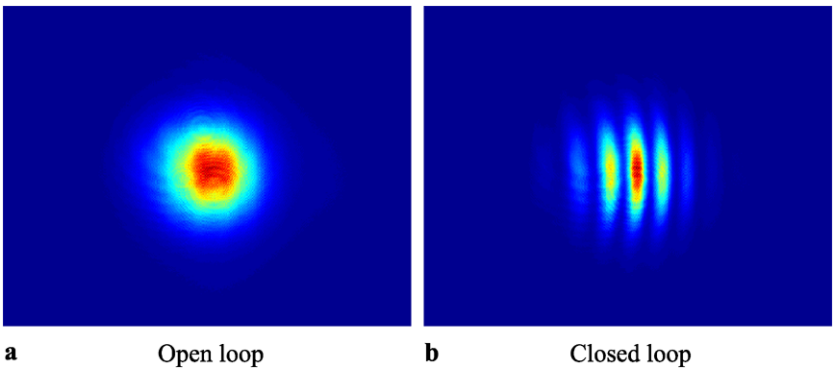

Fig. 4 Far-field intensity patterns for open loop and closed loop

In each channel, two phase modulators (PMs) are located before the pre-amplifier and after the main amplifier, respectively. All the fiber amplifiers and PMs used in this experiment are produced by our group. There are two fiber-coupled 5-mm-diameter beam collimators for the two beamlets and arranged conformally so that they can be combined on the target. One part of the collimated beams is transmitted to the CCD camera and the other is reflected to the target. Then part of the scattered light from the target surface is collected to the photodetector by the telescope. The photodetector is a PDA36A-EC Si amplifier detector with 400 nm–1100 nm response wavelength and 1.2-MHz bandwidth when the gain is at 10 dB, produced by THORLABS Corporation. The output signal of the photodetector travels to the controller for the phase controlling of PM2 and PM4. The controller also generates a modulating signal to PM1 or PM3. The CCD camera is used to observe the pattern of the phase-locking array. The single-dithering algorithm is implemented by Cyclone III produced by Altera Co. with a master frequency of 50 MHz.

In the experiment, firstly we tune the output power of each fiber amplifier to about 2 W. When the phase-control loops are open, the image on the CCD camera quickly moves, which is due to the fast-varying phase distortions or jitters coming from the fiber amplifier and the propagation path of the beamlets. Figure 3a is an image of the long-exposure pattern with open loop; the fringe contrast is about 12.7% obtained by taking the definition of the fringe contrast as $(I_{\max} - I_{\min})/(I_{\max} + I_{\min})$ with $I_{\max}$ and $I_{\min}$ representing the maximum optical intensity and the adjacent minimum on the pattern. When the phase-control loop B is closed, the image on the CCD camera becomes stable and

clear because the phase noise is mitigated effectively. Figure 3b shows the long-exposure pattern with closed loop; the fringe contrast is 74%.

When the output power is adjusted to about 10 W, the experimental results are shown in Fig. 4. Figure 4a and b show the long-exposure patterns with open loop and closed loop, respectively. When the phase-control loop is open, the fringe contrast of the long-exposure pattern is about 12%. After the loop is closed, the fringe contrast is about 73%.

It can be seen that in the experiment, the capability of TIL phase control almost did not degrade by increasing the laser power. In the main fiber amplifier stage, only two pump ports of the $(6 + 1) \times 1$ pump combiner are employed; increasing the pump power can further increase the laser power. We believe that TIL control based on the single-dithering technique can effectively compensate for the phase noises under much higher power conditions.

4 Conclusions

In summary, we have demonstrated a TIL adaptive phase-locked fiber laser array in high-power conditions with the single-frequency dithering technique. It is shown that the TIL phase-control system is capable of compensating for the high-power phase noises of the beams and improving the fringe contrast from 12% to 73% when the output power is about 20 W. In addition, it is straightforward to expand to dozens of channels with only one photodetector. With the number of fiber lasers in the array increasing, the serial working mode of the single-frequency dithering technique will diminish the system working bandwidth and impact the phase-locking effect of the laser amplifiers on the plane of the scattering surface. However, increasing the frequency of the modulation signal can alleviate this difficulty [23]. Besides, the experiment was carried out in the laboratory, so the time delay for the beams propagating from the laser array to the target is so short that we did not consider the dynamic effects of atmospheric turbulence on the TIL system in the experiment, which must be considered in further research. A TIL adaptive phase-locked fiber laser array with more than two channels, longer distance, and much higher power is undergoing testing to study it in detail.

References

1. D.J. Richardson, J. Nilsson, W.A. Clarkson, J. Opt. Soc. Am. B **27**, 63 (2010)
2. J.R. Leger, J. Nilsson, J.P. Huignard, A.P. Napartovich, T.M. Shay, A. Shirakawa, IEEE J. Sel. Top. Quantum Electron. **15**, 237 (2009)
3. T.Y. Fan, IEEE J. Sel. Top. Quantum Electron. **11**, 567 (2005)
4. T.M. Shay, J.T. Baker, A.D. Sanchez, C.A. Robin, C.L. Vergien, C. Zerinque, D. Gallant, C.A. Lu, B. Pulford, T.J. Bronder, A. Lucero, Proc. SPIE **7195**, 7195M-1 (2009)
5. B. He, Q.H. Lou, J. Zhou, J. Dong, Y. Wei, D. Xue, Y. Qi, Z. Su, L. Li, F. Zhang, Opt. Express **14**, 2721 (2006)
6. Z. Chen, J. Hou, P. Zhou, L. Liang, Z. Jiang, Acta Phys. Sin. **56**, 7046 (2007)
7. J. Wang, K. Duan, Y. Wang, Acta Phys. Sin. **57**, 5627 (2008)
8. Q. Peng, Y. Zhou, Y. Chen, Z. Sun, Y. Bo, X. Yang, Z. Xu, Y. Wang, K. Li, W. Zhao, Electron. Lett. **41**, 171 (2005)
9. X. Jia, F. Liu, S. Fu, Y. Liu, S. Yuan, X. Dong, Chin. Phys. B **16**, 2993 (2007)
10. P. Zhou, Z.J. Liu, X.L. Wang, Y.X. Ma, H.T. Ma, X.J. Xu, S.F. Guo, IEEE J. Sel. Top. Quantum Electron. **15**, 248 (2009)
11. L. Liu, M.A. Vorontsov, E. Polnau, T. Weyrauch, L.A. Beresnev, Proc. SPIE **6708**, 6708K-1 (2007)
12. J.E. Kansky, C.X. Yu, D.V. Murphy, S.E.J. Shaw, R.C. Lawrence, C. Higgs, Proc. SPIE **6306**, 63060G-1 (2006)
13. X. Chu, Z. Liu, Y. Wu, J. Opt. Soc. Am. A **25**, 74 (2008)
14. Y. Cai, Y. Chen, H.T. Eyyuboglu, Y. Baykal, Appl. Phys. B **88**, 467 (2007)
15. P. Zhou, X. Xu, Z. Liu, X. Chu, Acta Opt. Sin. **28**, 2051 (2008)
16. P. Zhou, Z.L. Chen, X.L. Wang, Chin. Opt. Lett. **7**, 39 (2009)
17. M.A. Vorontsov, V. Kolosov, J. Opt. Soc. Am. A **22**, 126 (2005)
18. M.A. Vorontsov, G.W. Carhart, M. Chen, G. Cauwenberghs, J. Opt. Soc. Am. A **17**, 1440 (2000)
19. T. Weyrauch, M.A. Vorontsov, T.G. Bifano, J.A. Hammer, M. Cohen, G. Cauwenberghs, Appl. Opt. **40**, 4243 (2001)
20. T. Weyrauch, M.A. Vorontsov, Appl. Opt. **44**, 6388 (2005)
21. M.A. Vorontsov, G.W. Carhart, Opt. Lett. **27**, 2155 (2002)
22. V. Jolivet, P. Bourdon, B. Bennai, L. Lombard, D. Goular, E. Pourtal, G. Canat, Y. Jaouen, B. Moreau, O. Vasseur, IEEE J. Sel. Top. Quantum Electron. **15**, 257 (2009)
23. Y. Ma, P. Zhou, X. Wang, H. Ma, X. Xu, L. Si, Z. Liu, Y. Zhao, Opt. Lett. **35**, 1308 (2010)
24. T.R. O'Meara, J. Opt. Soc. Am. **67**, 306 (1977)
25. T.M. Shay, Opt. Express **14**, 12188 (2006)
26. J.W. Goodman, J. Opt. Soc. Am. **66**, 1145 (1976)